

We are IntechOpen, the world's leading publisher of Open Access books Built by scientists, for scientists

4,800

Open access books available

122,000

International authors and editors

135M

Downloads

Our authors are among the

154

Countries delivered to

TOP 1%

most cited scientists

12.2%

Contributors from top 500 universities



WEB OF SCIENCE™

Selection of our books indexed in the Book Citation Index
in Web of Science™ Core Collection (BKCI)

Interested in publishing with us?
Contact book.department@intechopen.com

Numbers displayed above are based on latest data collected.
For more information visit www.intechopen.com



Fabrication of Two- and Three-Dimensional Photonic Crystals and Photonic Quasi-Crystals by Interference Technique

Ngoc Diep Lai¹, Jian Hung Lin², Danh Bich Do³, Wen Ping Liang⁴, Yu Di Huang⁵, Tsao Shih Zheng⁶, Yi Ya Huang⁷, Chia Chen Hsu⁸

¹*Laboratoire de Photonique Quantique et Moléculaire, UMR CNRS 8537, Ecole Normale Supérieure de Cachan,*

^{2,3,5,6,8}*Department of Physics, National Chung Cheng University, Chiayi 621,*

³*Department of Physics, Hanoi National University of Education, Hanoi,*

^{4,7,8}*Graduate Institute of Opto-Mechatronics, National Chung Cheng University, Chiayi 621,*

⁸*Department of Photonics, National Sun Yat-Sen University, Kaohsiung 804*

¹*France*

^{2,3,4,5,6,7,8}*Taiwan*

³*Vietnam*

1. Introduction

Photonic crystals (PCs) are composed of periodic dielectric or metallo-dielectric micro- or nano-structures that affect the propagation of electromagnetic waves in the same way as the periodic potential in a semiconductor crystal affects the electron motion (Joannopoulos et al., 1995; Sakoda, 2001). The wavelength ranges of disallowed propagation of electromagnetic waves of PCs are called photonic band gaps (PBG), which gives rise to distinct optical phenomena such as inhibition of spontaneous emission, high-reflecting omni-directional mirrors and low-threshold PC laser (Yablonovitch, 1987). Besides, the introduction of point or line defects into PCs offers many other potential applications, such as low loss waveguides, cavity resonators, and nanolasers, etc. (Noda et al., 2007; Rinne et al., 2008). The PCs with unique PBG properties therefore can be applied in a wide range of photonic and electronic devices (Inoue & Ohtaka, 2004). The major challenge for PCs study is the fabrication of these structures (Sibilia et al., 2008), with sufficient precision to prevent scattering losses blurring the crystal properties and with processes that can be robustly mass produced. Various techniques have been proposed to fabricate templates for PCs such as self-assembly of colloidal particles (Wong et al., 2003; Wu et al., 2008), holographic lithography (HL) (Berger et al., 1997; Campbell et al., 2000), and direct laser writing (Deubel et al., 2004; Sun et al., 1999), etc. Holographic lithography, in particular, is a very promising and inexpensive technique to fabricate large-area and defect-free PC templates. HL also allows to fabricate structures with unusual high levels of symmetry, called photonic quasi-crystals (PQCs) (Wang et al., 2003),

which recently attract a lot of attention since they have new optical properties that cannot be obtained with conventional PCs.

This chapter presents the fabrication and the characterization of two- and three-dimensional (2D and 3D) PCs and PQC templates. The fabrication is based on the multiple-exposure of two- and/or three-beam interference patterns. The optical properties of fabricated structures, such as pseudo PBG and diffraction patterns, are characterized and compared with theoretical calculations.

In Section 2, we demonstrate the fabrication of multi-dimensional periodic structures by the use of a new proposed multiple-exposure two-beam interference technique (Lai et al., 2005a). We show that different 1D, 2D and 3D structures could be created by applying multiple exposure of the two-beam interference pattern at appropriate orientations. Various 3D structures with a periodicity as small as 400 nm are experimentally obtained in agreement with theoretical calculations. This fabrication method presents a number of advantages over other holographic techniques based on three- or four-beam interference technique, such as, simple, low cost, and flexible, etc.

In Section 3, we propose various methods to embed desired defects into 2D and 3D periodic structures. Firstly, we combine the interference, presented in Section 2, with mask lithography technique in order to add long defects into 2D structures (Lai et al., 2005b). This combination has advantages such as simple and short fabrication time. Secondly, we demonstrate that a combination of the interference with the multi-photon polymerization direct laser writing permits to introduce a tiny and arbitrary defect into not only 2D but also 3D structures. Moreover, the defects could be patterned precisely into periodic structures with desired position and orientation by employing a double scanning microscopy technique (Lai et al., 2006a).

In Section 4, we investigate theoretically and experimentally the fabrication and the optical property of the QPCs. The fabrication also employs the multiple-exposure idea but it is applied to three-beam interference technique (Lai et al., 2006b). The fabrication of quasi-periodic structures with a rotation symmetry as high as 60-fold is demonstrated and confirms the theoretical calculation (Lai et al., 2007). Moreover, we calculate the optical property of fabricated quasi-periodic structures and demonstrate that PQC possesses an isotropic PBG that could not be achieved with traditional PCs.

In Section 5, we explore diverse non-desired effects existing in above mentioned interference technique, e.g., high absorption and photoacid diffusion or low concentration of the used photoresists, to fabricate 3D controllable thickness and 2D nano-vein structures. Here again, multiple-exposure two-beam interference technique is used for fabrication. The photoresist with high absorption at irradiated wavelength allows us to obtain 3D arbitrary structures by assembling multiple 1D or 2D structures. This technique is rapid and can produce very large structure with no limitation of number of layers, and with variable period and flexible design (Lai et al., 2010). Besides, by combining different kinds of photoresists, such as negative and positive ones, we demonstrate that 2D structures with nano-connection could be fabricated (Lai et al., 2009), which allows one to obtain better PBG, compared to traditional PCs.

Finally, we will make some conclusions of this work and show what this study brings to the fabrication of PCs and PQCs. We will also present some prospects.

2. Fabrication of PCs templates by multiple-exposure two-beam interference

2.1 Theoretical calculations

In this Section, we will demonstrate theoretically how a multi-dimensional interference pattern can be created by using multiple-exposure of two-beam interference pattern. Figure 1(a) shows a typical two-beam interference configuration. We assume that two laser beams of the same monochromatic plane wave source propagate in (x, z) -plane. In the overlapping area of two beams, they interfere and their total intensity is modulated in one-dimensional, as shown in Fig. 1b. If the plane containing two beams is rotated by an angle α around the z -axis (Fig. 1c), the 1D structure remains the same but its orientation changes with respect to α . When combining different 1D structures, which are oriented in different α angles, a 2D structure is obtained. Figure 1d shows an example of a 2D square structure created by two exposures at $\alpha = 0^\circ$ and $\alpha = 90^\circ$, respectively. In order to generate 3D periodic structures, we introduce a second rotation angle β as illustrated in Fig. 1e. The intensity distribution of a two-beam interference pattern in a sample oriented at angles α and β is expressed as

$$I_\alpha = 2E_0^2 \cos^2[kz \sin \theta \sin \beta + k \cos \theta \cos \beta(x \cos \alpha + y \sin \alpha)], \quad (1)$$

where $E_{10} = E_{20} = E_0$ are amplitudes of the electric fields of beams 1 and 2, respectively, k is the wave number, α and β are the rotation angles, and θ is the semi-angle between two beams. With a chosen couple of angles (α, β) , the 1D structure could be oriented in any direction in space. By combining multiple 1D structures with appropriate (α, β) -angles, we can fabricate any desired 3D periodic structure. Figure 1f shows as an example for a hexagonal close-packed-like structure structure created by three exposures of a two-beam interference pattern at $(\alpha, \beta) = (0^\circ, 30^\circ), (120^\circ, 30^\circ)$ and $(240^\circ, 30^\circ)$, respectively.

Note that this interference technique allows us to create any 2D and 3D structures, which cannot be created by three- or four-beam interference technique. Moreover, the lattice constants of the new created 3D structures are close in three dimensions for any value of θ -angle between two laser beams, that is difficult to be achieved by the commonly used one-exposure multi-beam interference technique (Campbell et al., 2000). The lattice constant of a two-beam interference pattern is determined by $\Lambda = \lambda/2\sin\theta$, where λ is the excitation wavelength.

2.2 Optical arrangement and fabrication process

Figure 2 shows the experimental setup of two-beam interference used to fabricate 1D, 2D and 3D periodic structures. A laser beam was first spatially cleaned and then extended to have a uniform and large profile. A 50/50 beam splitter was used to obtain two laser beams of the same profile, same polarization, and same intensity. Two mirrors were used to reorient the two beams in the position of the sample. These two beams interfered and their total intensity was periodically modulated in 1D in x -direction. The angle between two laser beams is denoted as 2θ and could be easily controlled by rotation of two mirrors. A sample was fixed in a double rotation stage, which could be rotated around the z -axis by an angle α and around the y -axis by an angle β .

Depending on the photoresist used and structure to be fabricated, we have used different kinds of excitation lasers, such He-Cd emitting at 325 nm and at 442 nm or Argon laser emitting at 514 nm. Those lasers are very stable and possess a long coherence length. According to excitation laser wavelength, different types of photoresists, negative and positive, have been used, such as SU8 and JSR (negative photoresists) and AZ4620 and S1818 (positive photoresists).

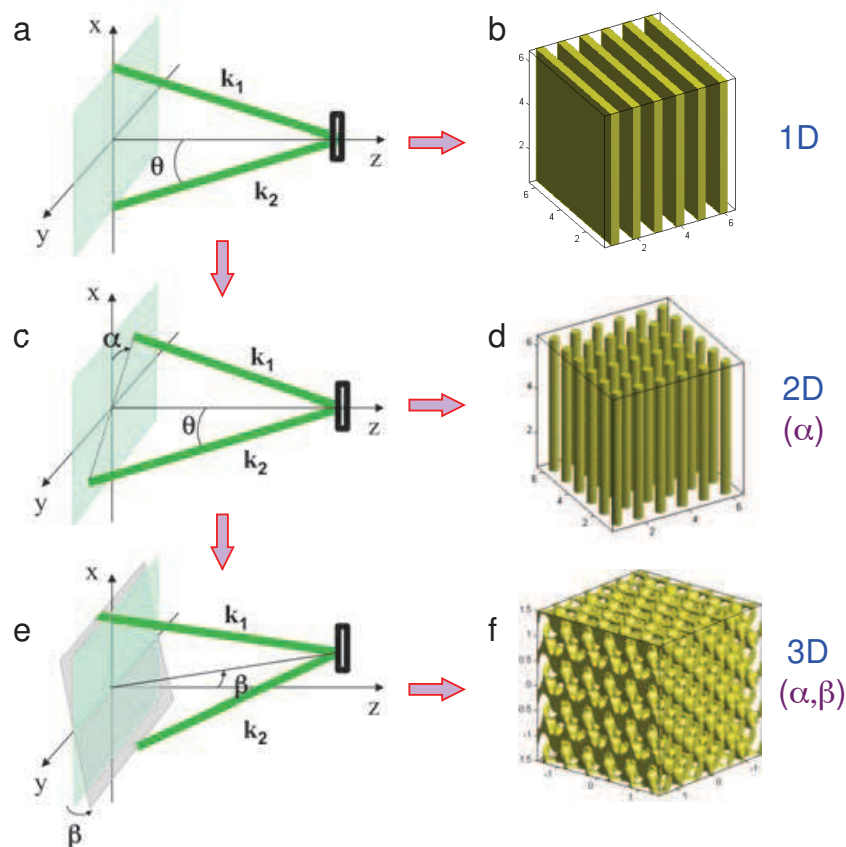


Fig. 1. Reorientation of two-beam interference pattern with multiple exposure allows to create one-, two- and three-dimensional micro and nanostructures. (c, d) 2D structures are obtained by two or three exposures at different orientation angles α . (e, f) Desired 3D structures are obtained by three or multiple exposures at different orientation angles α and β . Simulation examples of 1D (b), 2D square (d), and 3D hexagonal close-packed-like (f) structures.

The polymeric structure was fabricated following the procedures: i) preparation of thin film sample by spin-coating photoresist on glass substrate and pre-baking to remove the solvent; ii) exposure of interference pattern; and iii) post-baking and developing sample.

2.3 Fabrication results

Figure 3 shows the experimental result of various periodic structures obtained by one exposure, two exposures and three exposures of the two-beam interference pattern. The structures are very uniform for a large area corresponding to the laser beam size of about 1 cm^2 . A 1D structure was obtained by one exposure at $\alpha = 0^\circ$ as shown in Fig. 3a. 2D square (Fig. 3b) and hexagonal (Fig. 3c) structures were obtained with two exposures at $\alpha = 0^\circ$ and 90° and $\alpha = 0^\circ$ and 60° , respectively. Note that the hexagonal structure obtained by a double-exposure (Fig. 3c) consists of ellipsoidal dots (or holes). When applying three exposures with symmetrical orientations at $\alpha = 0^\circ$, $\alpha = -60^\circ$ and $\alpha = 60^\circ$, we obtained a 2D hexagonal structure with circular dots (or holes) as shown in Fig. 3d.

These structures were fabricated by using a negative SU8 photoresist (MicroChem. Corp.), with moderate film thickness ($1 \mu\text{m}$) and a laser beam at $\lambda = 325 \text{ nm}$. Similar results were also obtained by using positive AZ4620 or S1818 photoresist and a laser beam at $\lambda = 325 \text{ nm}$

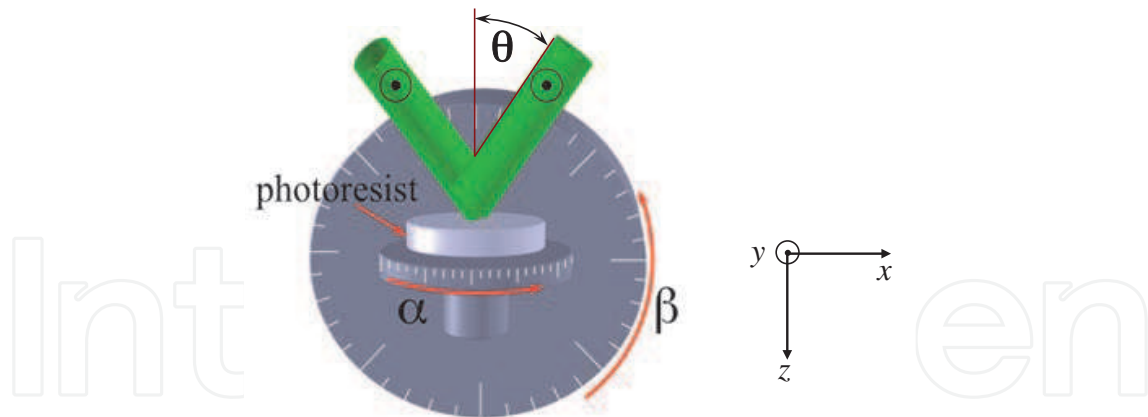


Fig. 2. Optical arrangement of multiple-exposure two-beam interference technique. Two laser beams of the same profile, polarization, and intensity were obtained by a 50/50 beam splitter. Two beams are then combined by using two mirrors, forming an angle 2θ . These beams interfere in the position of sample that is fixed in a double rotation stage: one can rotate around the z -axis, with an angle α , and the other can rotate around the y -axis, with an angle β .

or $\lambda = 442$ nm. Note that the structure obtained by using a negative photoresist is an exact duplication of the interference pattern, while the one obtained by a positive photoresist is an inverted duplication. These results are due to the chemical reaction happening when the resist absorbs the light, for which the negative resist forms a long polymer chain and the positive resist transforms from polymer chain to monomers. An intermediate situation in which the structure is not a duplication of the interference pattern will be presented in Section 5.3.

Note that using the same photoresist, either positive or negative, we were also able to fabricate 2D periodic structures with either material-dots or air-holes (Lai et al., 2005a), by controlling the exposure-dose, i.e., exposure-time or laser power. It is also important to know that by using this interference technique, one can easily adjust the lattice constant of the fabricated structure. The lattice constant can be as small as the half-wavelength of the excitation laser ($\Lambda_{\min} = \lambda/2$). In this work, we have fabricated periodic structures with lattice constant as small as 400 nm, obtained by using $\theta = 24^\circ$ and $\lambda = 325$ nm.

Figure 4 shows a 3D structure with a period of 400 nm. In order to fabricate a thick 3D structure, we need to choose a photoresist with low absorption at irradiation wavelength. We have therefore used another negative photoresist, namely JSR (thickness = $6 \mu\text{m}$), and an irradiation laser at $\lambda = 325$ nm. To obtain 3D periodic structures, we varied both α and β for different exposures. Many kinds of 3D structures were successfully fabricated by choosing appropriate α and β angles. An example of 3D structure shown in Fig. 4 was obtained by three exposures at $(\alpha, \beta) = (90^\circ, 0^\circ)$, $(0^\circ, 45^\circ)$ and $(180^\circ, 45^\circ)$, respectively. The experimental results show that 3D structures are uniform in large area and agree well with the simulation results. Moreover, comparing the lattice constants in top view and side view of 3D structures, we confirm that they are close in three dimensions as predicted by theory, which is impossible to achieve with four- or five-beam interference technique.

Figure 5a shows another 3D periodic structure of the same period $\Lambda = 400$ nm. This structure, called hexagonal close-packed-like, was obtained by three exposures at $(\alpha, \beta) = (0^\circ, 30^\circ)$, $(120^\circ, 30^\circ)$ and $(240^\circ, 30^\circ)$, respectively. With these 3D structures of small lattice constant, we expect to obtain a PBG in visible range. In order to characterize the optical properties of fabricated 3D structures, we simply sent a white light parallel beam into the

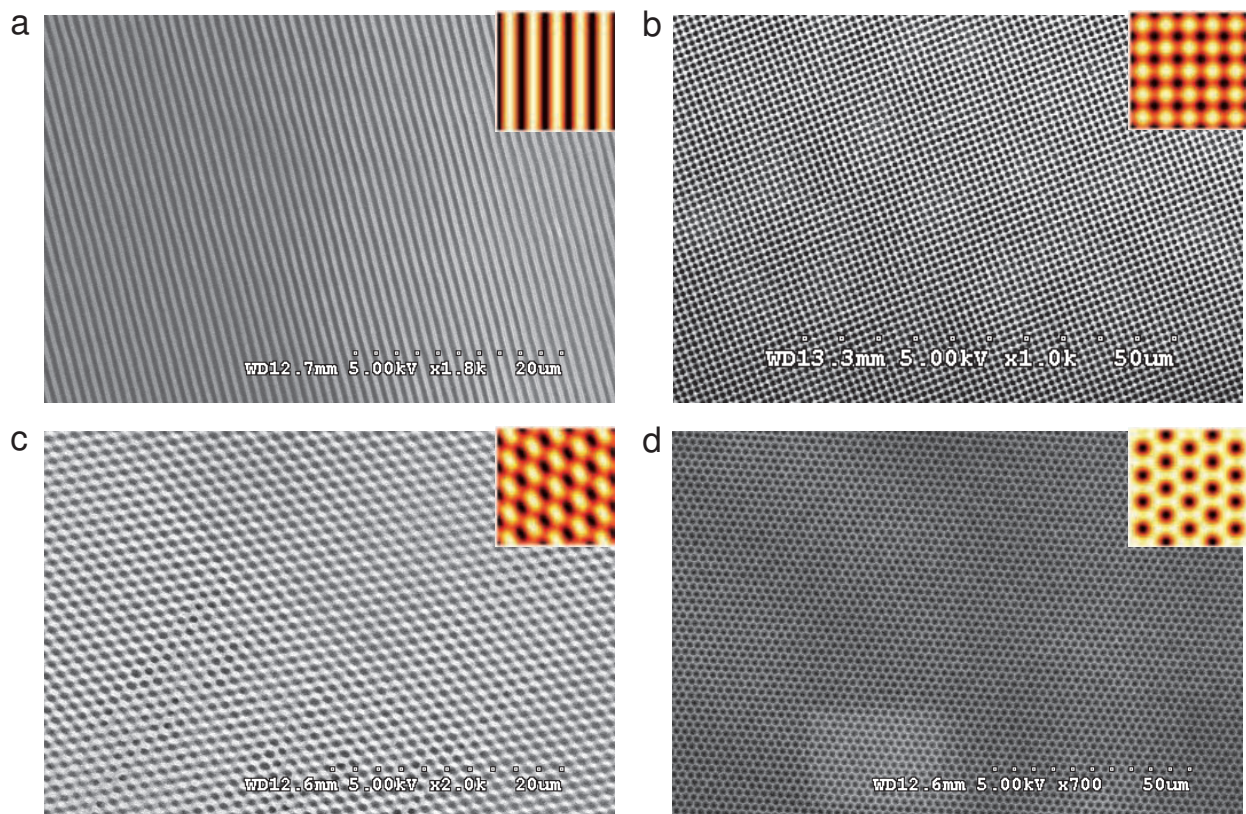


Fig. 3. SEM images of 1D and 2D periodic structures with a lattice $\Lambda = 1.1 \mu\text{m}$. (a) 1D structure obtained by one exposure. (b) 2D square structure obtained by two exposures at $\alpha = 0^\circ$ and $\alpha = 90^\circ$. (c) 2D hexagonal structure obtained by two exposures at $\alpha = 0^\circ$ and $\alpha = 60^\circ$. (d) 2D symmetric hexagonal structure obtained by three exposures at $\alpha = 0^\circ$, $\alpha = -60^\circ$ and $\alpha = 60^\circ$. Insets show simulation results of corresponding structures.

periodic polymeric structure and detected the reflection and transmission spectra. A typical result of spectra measured at normal incidence angle is shown in Fig. 5b. It is clear that there exists a reflection peak and a transmission dip at the same wavelength region, centered at 628 nm. When changing the incidence angle of the white light beam, this reflection peak (or transmission dip) was shifted to shorter wavelength and new reflection peaks (or transmission dips) appeared again in the visible domain. These peaks obviously correspond to a pseudo PBG of our fabricated periodic structures. However, theoretical calculation of the PBG of such new 3D holographic structure is still a challenge in order to confirm this experimental observation.

2.4 Discussion and conclusion

A simple optical interference method for fabricating 2D and 3D periodic structures is theoretically and experimentally demonstrated. This technique presents many advantages over others using multi-beam (three-, four-, or five-beam) interference: i) easy to fabricate desired 2D and 3D structures by simply rotating the sample for multiple exposures, ii) best contrast between the minimal and maximal intensities of interference pattern due to the identical polarization of two laser beams in the interference area, allowing one to fabricate 3D structure with small lattice constant, iii) new 3D periodic structures having the same period

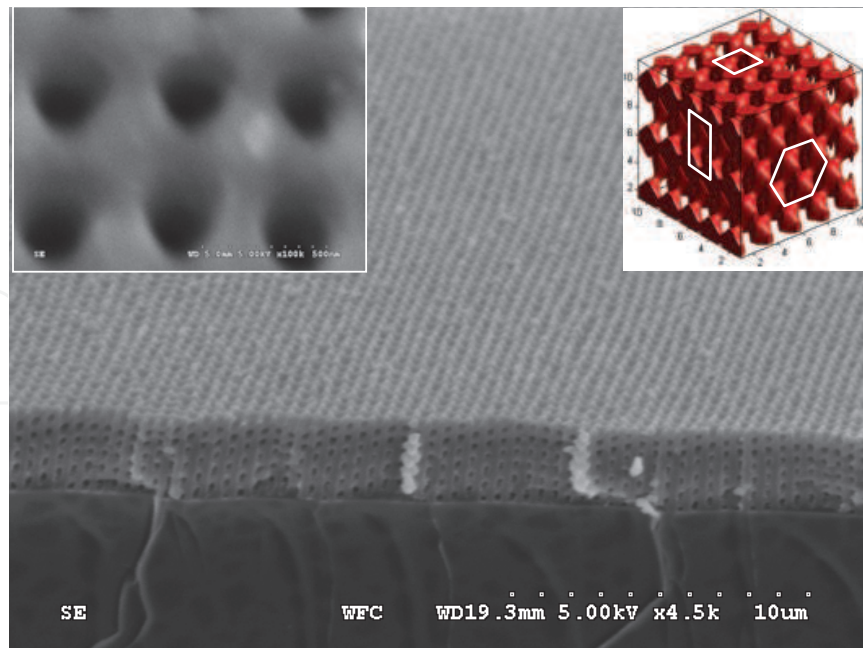


Fig. 4. SEM image of a 3D square/hexagonal periodic structure with a small lattice $\Lambda = 400$ nm, fabricated by three exposures with angles $(\alpha, \beta) = (90^\circ, 0^\circ), (0^\circ, 45^\circ)$ and $(180^\circ, 45^\circ)$, respectively. Left inset shows a zoom in of the top surface of the structure. Right inset shows a theoretical calculation for comparison.

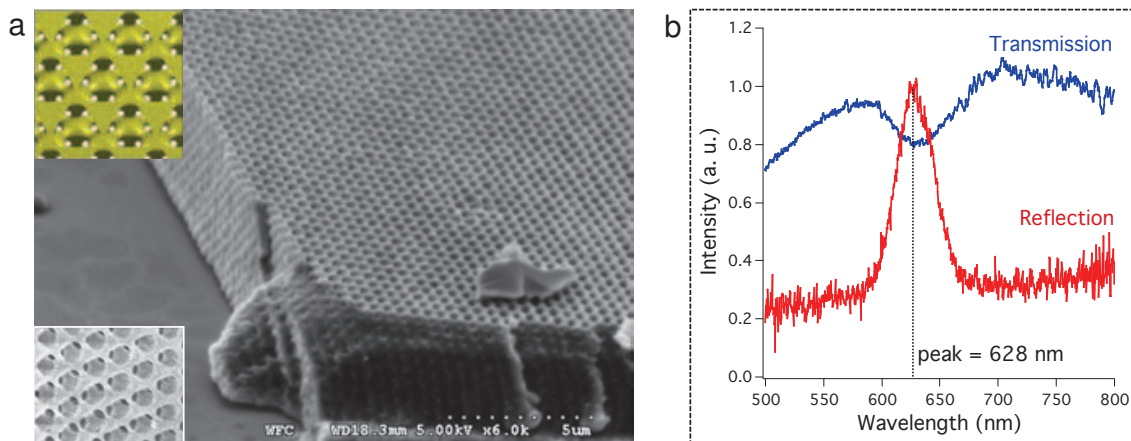


Fig. 5. (a) SEM image of a 3D hexagonal close-packed-like periodic structure with a small lattice $\Lambda = 400$ nm, fabricated by three exposures with angles $(\alpha, \beta) = (0^\circ, 30^\circ), (120^\circ, 30^\circ)$ and $(240^\circ, 30^\circ)$, respectively. Insets show a zoom in of the top surface of the structure and a corresponding simulation result. (b) Transmission and reflection spectra showing a clear photonic bandgap in visible range of the fabricated 3D structure.

in three dimensions, which can't be obtained by one-exposure of multi-beam interference technique.

Furthermore, this two-beam interference technique allows to fabricate not only periodic but also quasi-periodic structures (Gauthier & Ivanov, 2004). These structures recently attract a lot of attention and will be discussed in more detail in Section 4. Besides, we also can combine this interference technique with other fabrication techniques to fabricate large periodic structure containing desired defect, as it will be demonstrated in Section 3.

Finally, it is worth to note that although one theoretically can fabricate a periodic structure with a $\Lambda_{\min} = 162.5$ nm (the excitation wavelength is 325 nm), it's still difficult to obtain a good 3D periodic structure with periodicity smaller than 300 nm. This difficulty can be explained by the fact that when the structure lattice is small, the photoacid diffusion of used photoresist (Juodkazis et al., 2005) makes the structure features connecting all together, and they cannot be separated by the developing process. This is true for all optical lithography techniques used to fabricate photoresist-based nanostructures. Indeed, multiphoton polymerization direct laser writing, for example, can create individual spots with a feature size down to 120 nm (Kawata et al., 2001), but structures were connected together when spots were closely created (Park et al., 2005). Improvement of photoresist quality is a challenge in order to fabricate 3D polymeric structures with nano lattice constant.

3. Incorporation of well-defined defects into periodic microstructures

The use of interference technique allows to fabricate large and uniform periodic structures containing no defect. However, there are considerable interests to embed desired defects into 2D and 3D periodic structures. The introduction of point or line defects into PCs offers various potential applications, e.g., low-loss waveguides, cavity resonators and microlasers, etc. (Noda et al., 2007; Rinne et al., 2008).

In this Section, we present different techniques, that can be combined with two-beam interference technique to embed desired defects into 2D and 3D periodic structures.

3.1 Creation of large defect by mask optical lithography

In order to rapidly and simply introduce arbitrary defects into 2D PCs, we have used a combination of HL technique and mask-photolithography technique as an efficient method to produce large-area PC templates with desired long defects. To fabricate periodic structures, we used multiple-exposure of two-beam interference pattern to produce various 2D periodic square or hexagonal structures. The sample was exposed but not developed at this stage. Desired defects were then introduced in these pre-fabricated structures by irradiating the sample with a large and uniform beam of the same laser through a mask in which the designs of desired defects were patterned [Fig. 6a]. The sample was finally developed to obtain a 2D periodic structure containing desired defect.

Note that solid or air-gap type of defect can be obtained depending on the choice of photoresist. For a negative photoresist, a solid type of defect is obtained. On the other hand, for a positive photoresist, an air-gap defect is obtained. Figure 6b shows an example of a 2D periodic square structure containing a line defect. This structure was obtained by using a positive photoresist AZ-4620 (Clariant Corp.). This photoresist absorbed a UV light pattern (interference pattern and mask) and became soluble. After developing process, we obtained a periodic structure made of AZ photoresist embedded with desired air-defects.

Using this combination technique, we can generate whatever types of defect (point defect, waveguide, Mach-Zehnder, etc.) with the size varying from several micrometers to several centimeters into periodic structures. Furthermore, we can control their positions and orientations with respect to periodic structure. Indeed, by using the multiple-exposure of two-beam interference, we were able to control perfectly the orientation of the periodic 2D structures. With well-known orientation of the defect design in the mask, we therefore could embed the defects into the periodic structures in the desired directions. The defect shown in Fig. 6b was created, for example, at 45° with respect to the orientation of the square structure.

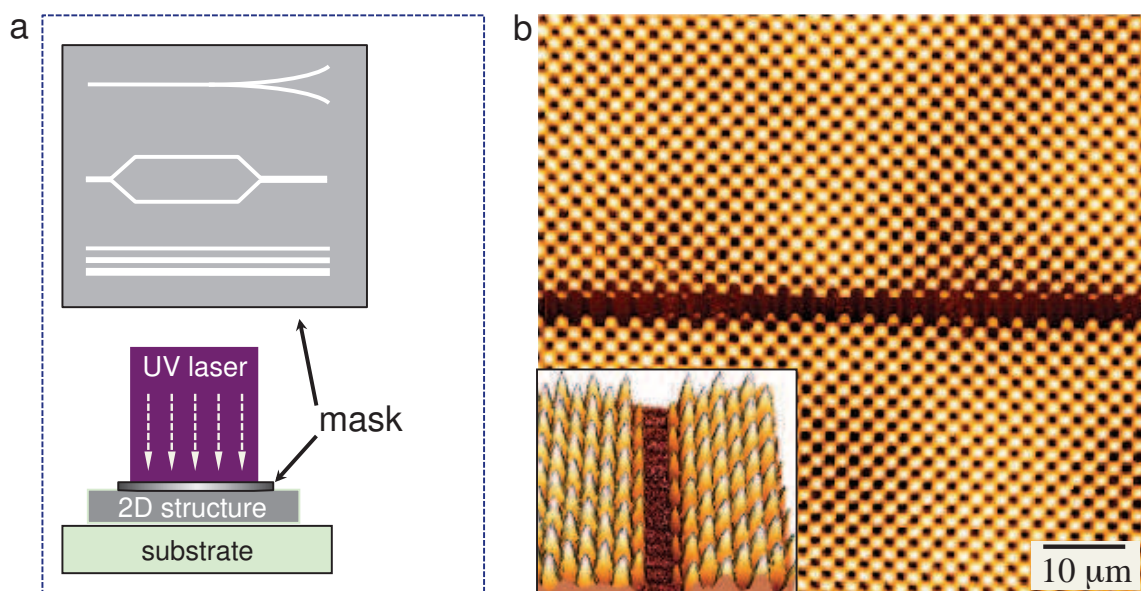


Fig. 6. (a) Creation of large defects into 2D periodic structures by optical mask-lithography. 2D structures are fabricated by two-beam interference technique. Before developing 2D structures, desired defects, which are designed in a mask, are introduced into 2D structures by an uniform beam. The sample is finally developed to obtain the desired structure. (b) AFM images of a 2D square periodic structure embedded with a line defect. The line defect is oriented at 45° with respect to the orientation of the square structure.

3.2 Introduction of small arbitrary defects by multiphoton polymerization technique

In order to create small defects with flexible design, we have combined the two-beam interference technique with the multiphoton polymerization direct laser writing technique (Deubel et al., 2004; Sun et al., 1999). The periodic structure was first created by the multiple-exposure two-beam interference. The tiny desired defect was then introduced into the periodic structure by the direct laser writing process. For the later step, a Ti:Sapphire laser with 830 nm - central wavelength, 100 fs - pulse duration, and 80 MHz - repetition rate was used as the light source to induce multiphoton polymerization effect. The laser beam was tightly focused into the sample by using a high numerical aperture (NA) objective lens (OL, NA = 0.95). The multiphoton absorption could be realized only at focusing region, which then induces the polymerization or depolymerization effect. The diameter of polymerized/depolymerized spot at focal region of OL can be continuously controlled by adjusting the laser power or exposure time. In our case, the smallest diameter of polymerized/depolymerized spots was about 200 nm. The sample could be translated in three dimensions (x, y, z) by a piezoelectric translation (PZT) stage with 10 nm-resolution [Fig. 7a]. The desired defects were designed by a computer software that commanded the voltage applied to the PZT stage.

Here again, either negative or positive photoresist can be used to fabricate various types of defects. Figure 7b shows a 2D periodic hexagonal structure containing some arbitrary "letters" defects, obtained by using a negative SU8 photoresist. The result shows that we can fabricate any periodic structure containing defect as desired. Figure 8 shows the result of a 3D structure containing some "line" defects. The 3D structure was obtained by three exposures at $(\alpha, \beta) = (0^\circ, 30^\circ), (60^\circ, 0^\circ)$ and $(180^\circ, 0^\circ)$. The defects were introduced into the 3D structure at different z -positions as indicated in Fig. 8a. The electronic microscope doesn't allow to

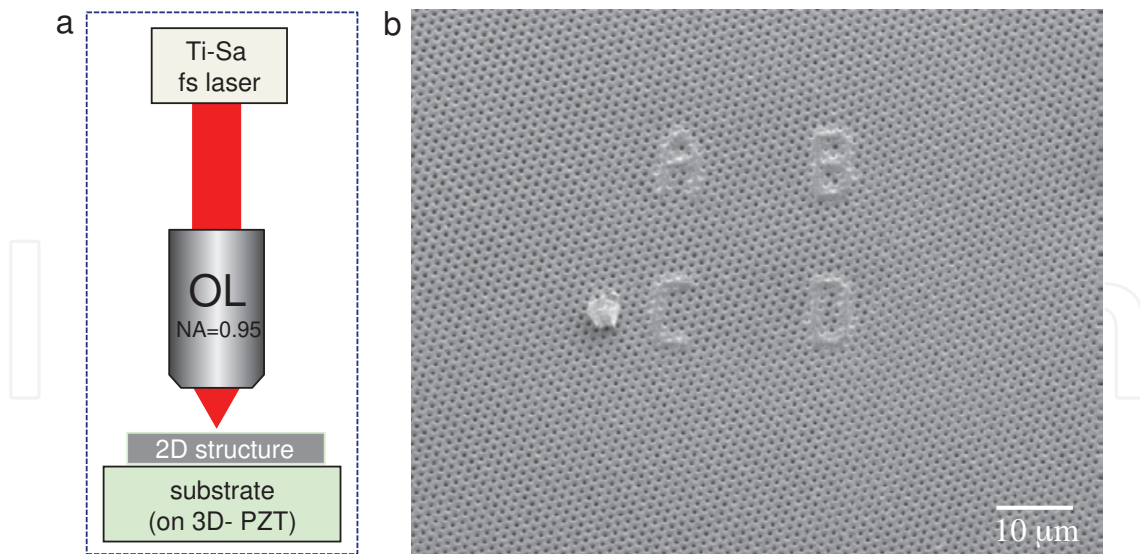


Fig. 7. (a) Simple optical arrangement of a multiphoton laser microfabrication system used to pattern arbitrary defects into periodic structures. 2D structures are fabricated by two-beam interference technique and desired defects are patterned by multiphoton polymerization direct laser writing technique. (b) SEM images of a 2D hexagonal periodic structures ($\Lambda = 1.15 \mu\text{m}$) embedding different letters defects. Note that the small particle near the letter C is a small piece of glass accidentally dropped in the structure during the cutting process of the sample.

observe all defects, in particular those created inside the 3D structure. However, thanks to the fabrication technique and the 3D structure design, we confirm the creation of defects (Z4 for example) at the predicted position and orientation inside 3D periodic structure.

Note that, since the defect was introduced into the pre-fabricated periodic structure before the developing step (the periodic structure information is unknown yet), the position and orientation of fabricated defect with respect to the periodic structures were not totally controlled. It requires a technique to precisely incorporate the desired defects into the periodic structures.

3.3 Precise introduction of desired defects by a double-scanning technique

We have therefore developed a double-step laser scanning technique to embed arbitrary defect in periodic structures with desired position and orientation. We first determined the position and orientation (the mapping step) of periodic structure, and then embedded the desired defects (the fabrication step) into the periodic structure with well-known position and orientation. For both steps, we have used the same direct laser writing system but with different excitation laser powers.

The main concept of the mapping step is based on the shrinkage effect of the negative photoresist. In fact, when excited by two-beam interference pattern, the SU8-monomers moved from the low intensity area to the high intensity area to form linked polymer chains. This induced a 2D surface relief grating (SRG) of the photoresist sample. The SRG image obtained by atomic force microscope, without developing process, is shown in Fig. 9a indicating a modulation of sample surface of about 30 nm. When using a low excitation power of femtosecond laser and detecting the transmission light, we obtained a similar image of the 2D non-developed structure [Fig. 9b]. In this step, the excitation power was chosen to be

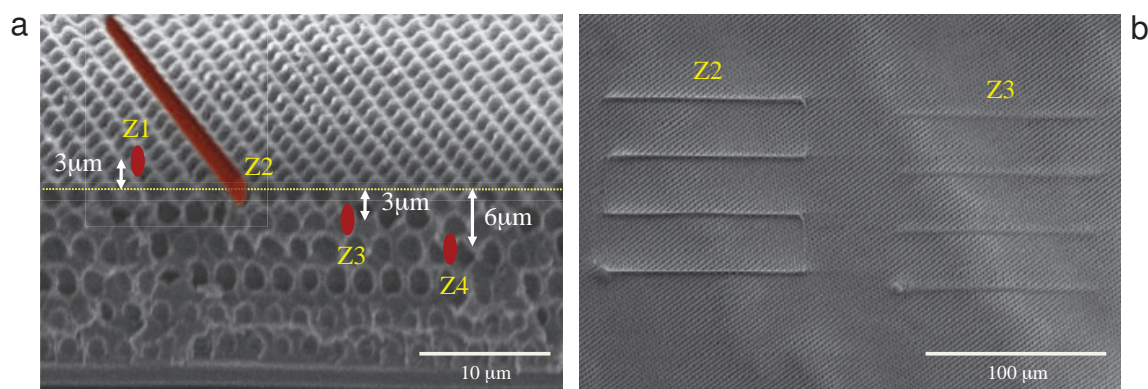


Fig. 8. Introduction of arbitrary defect into a 3D periodic structure by multiphoton polymerization direct laser writing technique. (a) SEM image of the 3D structure and illustration of recording defects at different vertical positions. 3D structures were created by three exposures of two-beam interference pattern. Desired defects were introduced into 3D structures by direct laser writing technique. (b) SEM image of a 3D hexagonal/hexagonal periodic structures ($\Lambda = 2 \mu\text{m}$) embedding several line defects. Only defects on the surface (Z2) and $3 \mu\text{m}$ below of the structure surface (Z3) can be observed by SEM. The Z1 is not fabricated since the focusing point of the direct laser writing technique was out of the structure surface. The Z4 is not observed because it is too deep inside the sample.

lower than the threshold of multiphoton absorption effect so that the mapping process didn't induce any polymerization effect.

Using the scanned image, the position and orientation of the periodic structures were then determined. By keeping the sample unmoved, the desired defects were patterned in the designed positions and orientations with respect to the periodic structures [Fig. 9b]. For this fabrication step, the excitation laser power was increased to induce the multiphoton absorption polymerization at the focused beam. The defect was then created by scanning the focusing point following the defect design with accurate position and orientation. Figure 9c shows a SEM image of a 2D square periodic structure containing some 90° -bending defects, which agree well with the defects design shown in Fig. 9b.

In a similar way, we expect that this double-scanning technique could be applied to introduce precisely desired defects into 3D periodic structures. In this case, the surface of 3D periodic structure is also modulated due to the shrinkage effect as in the case of 2D periodic structures. By scanning only the structure surface, we can get informations (position and orientation) of the surface of the studied 3D structures. Because no intermediate development is needed before mapping, the fabricated defect-free periodic structures should be exactly identical to its design. The position and orientation of structures below the surface at any z -position could be therefore determined by using the design of fabricated periodic structures. The desired defects can then be introduced at accurate positions and orientations inside 3D periodic structures.

4. Study of 2D and 3D quasi-periodic structures

Multi-beam interference technique (Wang et al., 2003) is a commonly adopted HL method to fabricate a 2D quasi-periodic structure (QPS). This technique however demands a careful alignment of multiple laser beams, which is a challenge for experimental fabrication. In this Section, we demonstrate theoretically and experimentally that combination of three-beam

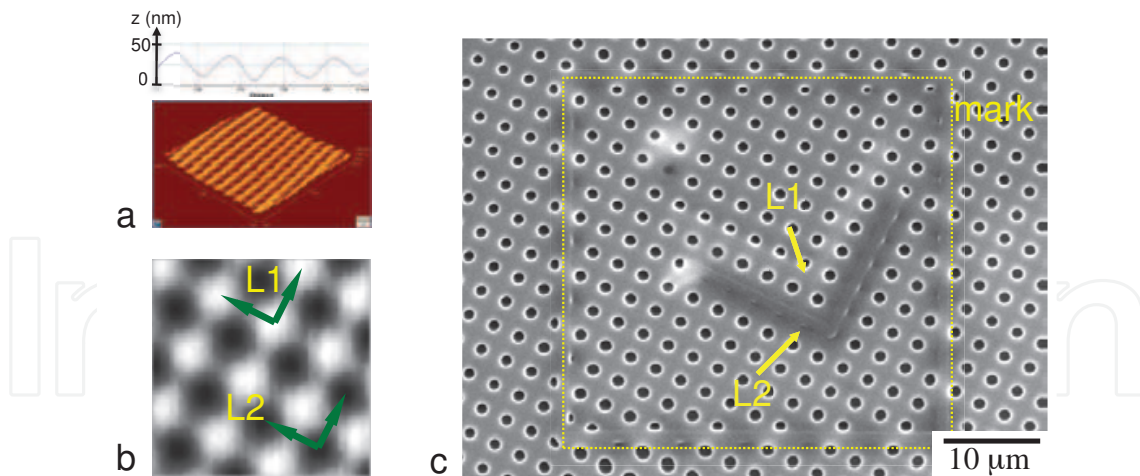


Fig. 9. Precise introduction of desired defect into periodic structure. 2D square structure is obtained by exposing the sample by a double exposure of a two-beam interference pattern at $\alpha = 0^\circ$ and $\alpha = 90^\circ$. (a) AFM image of a structure obtained without developing step. The structure can be seen thanks to the shrinkage effect of negative photoresist. (b) The structure is mapped by using a direct laser writing at low excitation power, and its position and orientation are identified. (c) SEM image of a 2D structure containing well-defined defect. Note that the defect L1 is invisible since it is overlapped with the solid part of the periodic structure. The large square frame around defect is added intentionally for identification of defect.

interference technique and multiple-exposure idea is a simple and useful method to fabricate various kinds of 2D and 3D QPS with very high rotation symmetry level.

4.1 Optical arrangement of multiple-exposure three-beam interference

Figure 10 shows the experimental arrangement used to fabricate 2D and 3D QPSs. To avoid alignment complexity and inaccuracy as well as mechanical vibration instability, a single multi-surface prism was employed. A large and uniform beam is sent in normal incidence upon three surfaces of the prism, noted as A_1 , A_2 , and A_3 [Fig. 10a]. After passing through the prism, three sub-beams corresponding to three surfaces are obtained and deviated symmetrically around the O-axis. Each beam makes an angle θ with respect to the symmetrical O-axis. They are then overlapped at one point in which the total intensity is periodically modulated due to their interference. The interference pattern of three laser beams is a 2D hexagonal structure (6-fold symmetry). A photoresist sample could be placed at the cross-point of three beams and the interference pattern could be recorded to the sample.

In order to fabricate 2D QPSs, the sample holder is aligned perpendicular to O-axis [Fig. 10b] and the sample could be rotated around this axis by an angle α for different exposures. To fabricate 3D QPSs, the sample surface (N-axis) is oriented by an angle β with respect to O-axis [Fig. 10c] and the sample could be rotated around the z-axis by an angle α for different exposures. By this way, we can easily make multi-exposure of the interference pattern to fabricate desired multi-fold symmetry 2D QPSs. Indeed, by making for example a double-exposure and a triple-exposure of the three-beam interference pattern with appropriate rotation angles, we can fabricate 2D and 3D twelve-fold QPSs, respectively. Insets of Fig. 10b and Fig. 10c show simulation results of those QPSs.

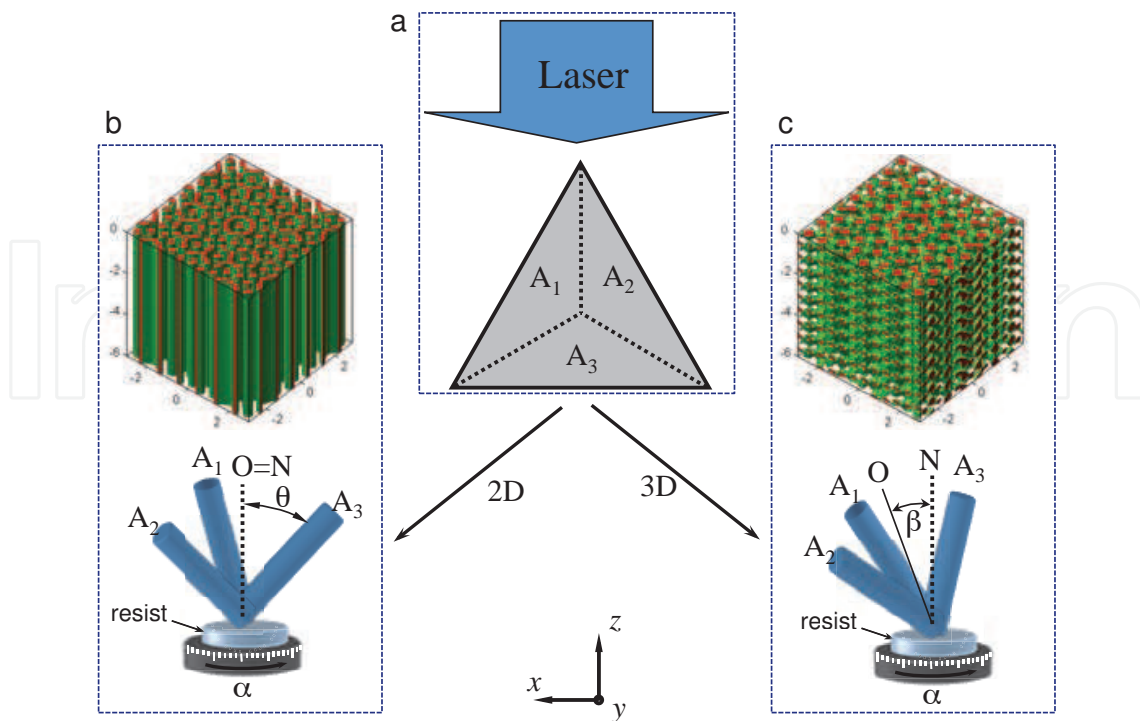


Fig. 10. Fabrication of quasi-periodic structure by multiple-exposure of three-beam interference pattern. (a) A large and uniform laser beam comes into a multi-surface prism along the z -axis and it is divided into three sub-beams corresponding to three surfaces denoted as A_1 , A_2 , and A_3 , respectively. Three beams after passing through the prism changed their directions and overlapped at one point in the z -axis in which a photoresist sample was placed for the fabrication. (b) If the symmetrical axis (O) of the three beams is parallel to the normal axis (N) of the sample, we can fabricate different 2D quasi-periodic structures by exposing the sample at different rotation angles, α . (c) If O -axis makes an angle, β , with N -axis, we can fabricate different 3D quasi-periodic structures by applying multiple exposures.

4.2 Fabrication of highly rotational symmetric 2D quasi-periodic structures

To fabricate large QPSs, we have used a large and uniform laser beam emitted from a He-Cd laser ($\lambda = 442$ nm), which was spatially cleaned and extended (diameter = 2 cm) by a lenses and pinhole system. A mask with three irises was introduced in the laser beam to select three laser sub-beams of the same profile (diameter = 6 mm) and same intensity. These beams are sent to three surfaces, A_1 , A_2 , and A_3 of the prism to realize the three-beam interference. The sample (AZ4620 photoresist, thickness = 1 μm) is fixed in a holder and can be oriented by angles α and β .

To fabricate 2D QPSs, the β is chosen to be 0° , i.e., the O -axis and the N -axis are parallel. The sample is rotated at different α angles for multiple exposures. Figure 11a shows the experimental results of a 2D QPS obtained with three exposures of the three-beam interference pattern at $\alpha = 0^\circ$, 20° and 40° , respectively. The structure is quite uniform in a very large area (6 mm \times 6 mm, corresponding to the size of the iris). Inset of Fig. 11a shows a zoom in of a particular area of the QPS in which one can clearly see a 18-fold symmetry structure, in agreement with the theoretical calculation. This symmetry is confirmed by measuring the diffraction pattern of fabricated structure. Figure 11b shows the corresponding diffraction pattern of the 2D QPS, which contains a series of circles constituting by eighteen bright spots

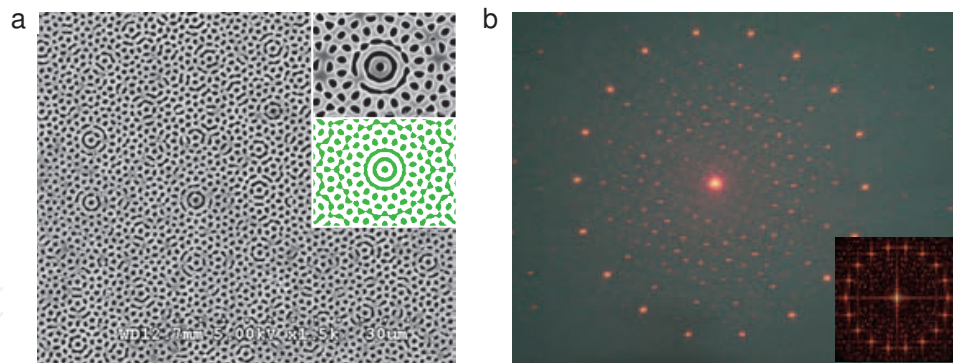


Fig. 11. (a) SEM image of a 18-fold symmetry structure that is fabricated by three exposures of three-beam interference pattern with $(\alpha, \beta) = (0^\circ, 0^\circ), (20^\circ, 0^\circ)$ and $(40^\circ, 0^\circ)$. Insets show theoretically and experimentally a zoom in of a particular area that shows the 18-fold symmetry level of the structure. (b) Experimental diffraction pattern of the corresponding fabricated structure. Inset shows the calculated Fourier transform of the 18-fold symmetry quasi-periodic structure.

around the zero-order diffraction spot. We also calculated the Fourier transform of this 18-fold QPS and found that the spectrum, as shown in inset of Fig. 11b, and its 18-fold rotation symmetry, inherited by the statistical symmetry of the structure, is clearly visible.

We have fabricated by this technique many other QPSs structures with the rotation symmetry level as high as 60-fold. The rule applied for the number of exposure and the symmetry level of QPSs is defined by :

$$N = 6n \quad (2)$$

and

$$\alpha_i = 60(i - 1)/n, \quad (3)$$

where N is the rotation symmetry level, α_i is the angle corresponding to the i th-exposure, and n is the number of exposures.

4.3 Fabrication of 12-fold symmetry 3D quasi-periodic structures

For fabrication of 3D QPSs, we reoriented the symmetrical O-axis of three laser beams with respect to the z-axis by an angle β [Fig. 10c] and made three exposures of the three-beam interference pattern with $\alpha_i = 0^\circ, 20^\circ$ and 40° , respectively. The β -angle was chosen to be 54.7° for all exposures. With this β -angle, the rods of the hexagonal structure obtained by one-exposure are perpendicular to the rods of the hexagonal structure obtained by any other two exposures. The combination of three hexagonal structures oriented in three perpendicular directions resulting in a 12-fold symmetry 3D QPS, as previously seen in Fig. 10c. AZ4620 positive photoresist with a thickness = $12 \mu\text{m}$ was chosen to fabricate these structures. Figure 12a shows a SEM image of a 3D QPS fabricated by the above mentioned parameters. Quasi-periodic structure can be clearly seen in the top surface. Inset of Fig. 12a shows a side view (tilt angle 60°) of this 3D QPS in which we can see that the structure is also quasi periodic in the z-direction. Remark that the 12-fold symmetry can be seen in the xy -plane (not xz -neither yz -plane) and other seven planes as illustrated in middle inset of Fig. 12a. These eight planes are oriented in four different directions making the structure quasi-periodic in 3D.

A beautiful diffraction pattern with very bright spots was also obtained showing a 12-fold symmetry level in the xy -plane of the fabricated structure [Fig. 12b]. To experimentally prove

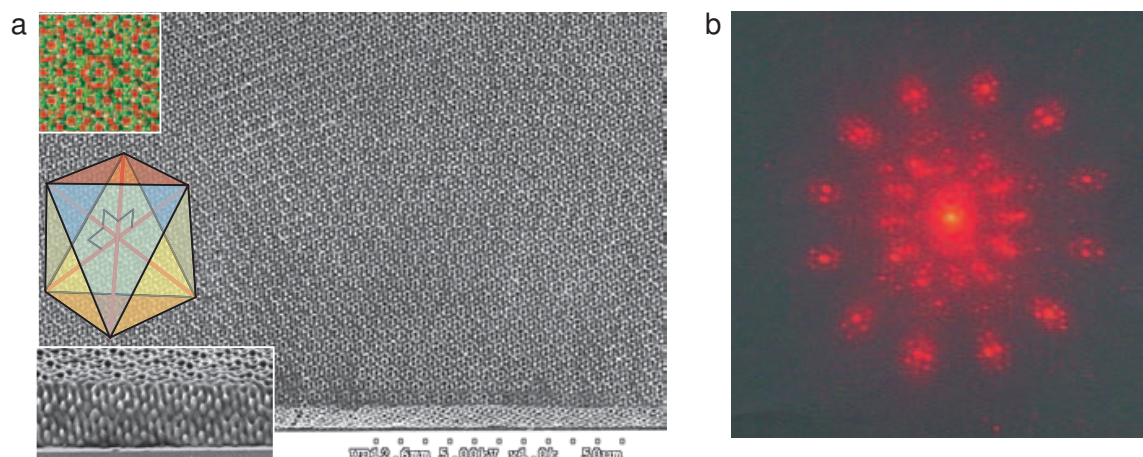


Fig. 12. (a) SEM image of a 3D quasi-periodic structure that is fabricated by three exposures of three-beam interference pattern with $(\alpha, \beta) = (0^\circ, 54.7^\circ), (120^\circ, 54.7^\circ)$ and $(240^\circ, 54.7^\circ)$. The upper inset shows a theoretical calculation of the top surface of the structure and the lower inset shows a zoom in of the side view of the structure. The middle inset illustrates 8 equivalent planes in which we can identify the 12-fold symmetry of structure. (b) Experimental diffraction pattern of the corresponding fabricated structure, showing a complicated distribution of a 3D quasi-periodic structure.

the symmetry level of other seven planes, it is worth to mention that the sample is not thick enough to check the quasi-structure from side view by SEM or to send a laser beam to one side of the sample to observe the diffraction pattern. However, the diffraction pattern shown in Fig. 12b is more complicated than those of 2D QPSs and it should reflect an interesting property of these 3D QPSs.

Furthermore, our calculations predicted that 12-fold symmetry 3D QPS can also be obtained by six exposures with $\beta = 54.7^\circ$ and $\alpha_i = 0^\circ, 30^\circ, 120^\circ, 150^\circ, 240^\circ$ and 270° , respectively. In that case, the 12-fold symmetry structure could be seen in sixteen equivalent planes and the PBG of such structure must be more isotropic in 3D.

4.4 Calculation of transmission spectra of 2D quasi-periodic structures

There exists many calculation methods for analyzing PBG properties of PCs. To use those calculation methods, the PC structure needs to be periodic and can be represented by an unit cell structure. However, in the case of QPSs it doesn't exist such unit cell structure, therefore PBG calculation is almost impossible. In some particular cases of QPSs, such as Penrose structure (Zoorob et al., 2000), one needs to use so-called supercell structure to calculate and it takes a long simulation time and large computer memory.

In general, the optical properties of QPSs could be characterized by calculating the transmission or reflection spectra of a light beam applied to the QPSs. For the QPSs fabricated by the multiple-exposure three-beam interference technique, the 2D approximation finite element method (FEM) (Lai et al., 2006b) was used to simulate the transmission spectra for different incident angles. For that we sent a broad-band light source into a finite size quasi-structure at different incidence angles and measured the transmission spectra. The QPSs fabricated by interference technique however contains some particular areas with a rotation symmetry as shown in Fig. 11a. We therefore calculated the transmission spectra using different finite-size structures with and without this symmetrical center. Figures 13 and 14 show the transmission spectra of a 2D 24-fold QPS, for two different cases, with and

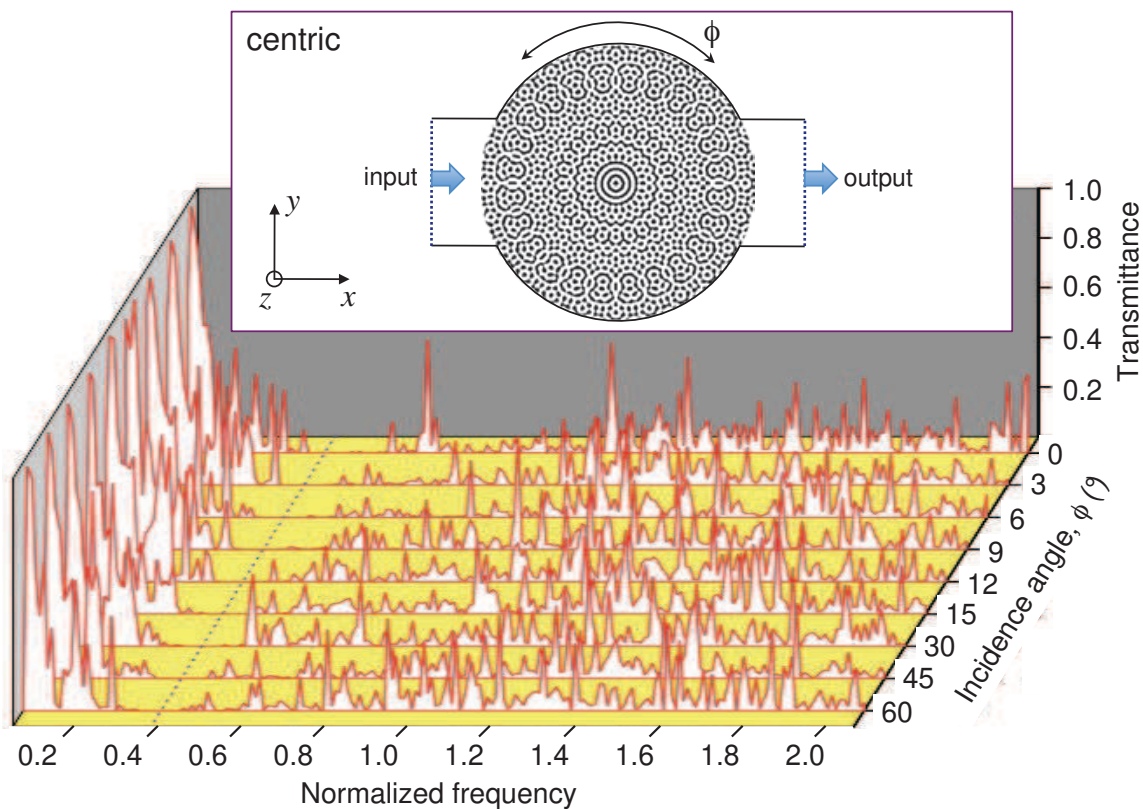


Fig. 13. Simulation result of transmission spectra (TM-mode) of a 2D 24-fold symmetry quasi-periodic structure. The structure is obtained by four exposures of three-beam interference pattern at $(\alpha, \beta) = (0^\circ, 0^\circ), (15^\circ, 0^\circ), (30^\circ, 0^\circ)$ and $(45^\circ, 0^\circ)$. The calculation is realized using a particular area containing a symmetric point, and the transmission spectra are calculated with different incident angles, ϕ , of the light beam. An isotropic photonic bandgap centered at 0.4 is clearly observed.

without symmetry center. The 24-fold symmetry structure was obtained by four-exposure of three-beam interference pattern at $\alpha_i = 0^\circ, 15^\circ, 30^\circ$ and 45° , respectively. The used finite-size structure is shown in each corresponding calculation result. For all calculations, we assumed that the refractive index of the structure material and the air are 1.6 and 1, respectively. A transmission dip is observed between 0.35 and 0.45 normalized frequency, which corresponds to the PBG of the structure. Because the lowest symmetry level of these QPSs is six-fold, according to a hexagonal structure obtained by one exposure, it is enough to calculate the transmission spectra only for the incidence angles ranging from 0° to 60° . The calculation result shows that the transmission spectra obtained with different light incidence angles are almost the same, corresponding to an isotropic PBG.

5. Fabrication of 2D nanovein structures and 3D controllable-thickness structures

Through the above presented work, the working principle of HL technique can be summarized as follows: a photoresist is placed in the interference region and the interference pattern is transferred into the photoresist to form a corresponding matter structure. The photoresist is subsequently developed and the periodic or quasi-periodic structures are then obtained. However, in this simple argument, some factors that may affect fabricated structures are ignored. Indeed, many researches have shown that final fabricated structures obtained by HL

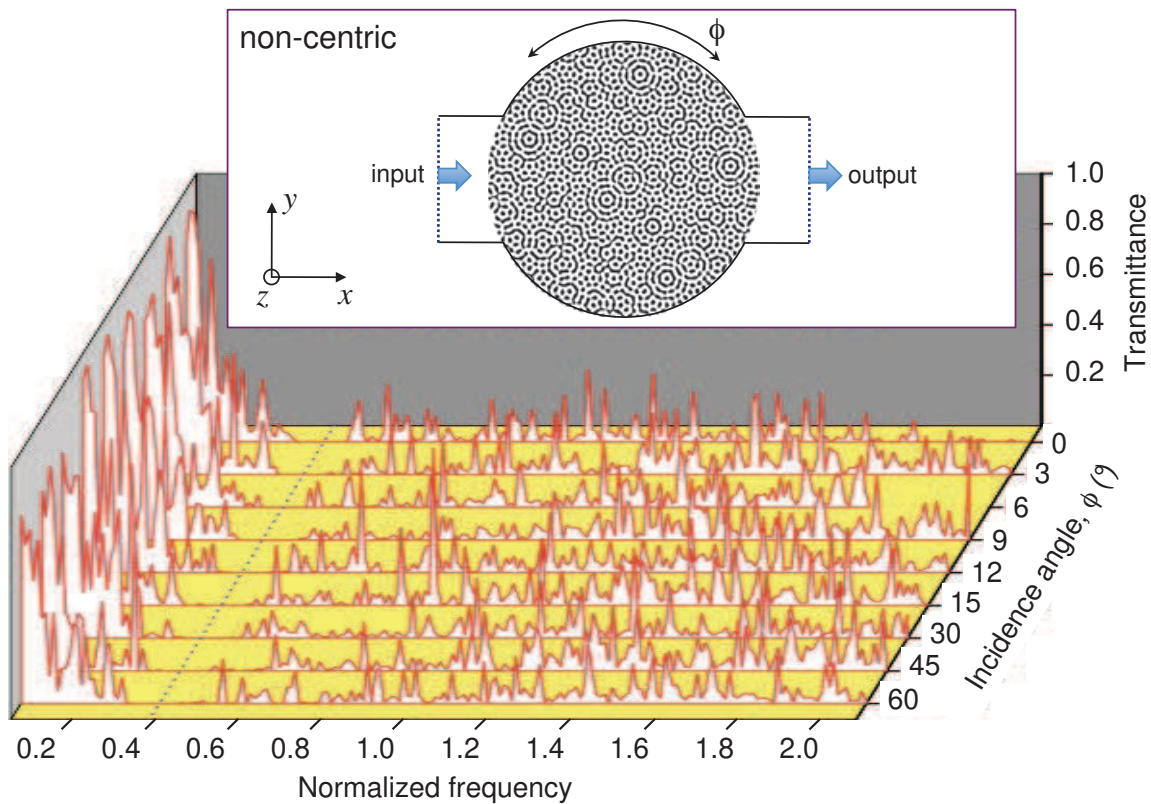


Fig. 14. Simulation result of transmission spectra (TM-mode) of a 2D 24-fold symmetry quasi-periodic structure. The structure is obtained by four exposures of three-beam interference pattern at $(\alpha, \beta) = (0^\circ, 0^\circ), (15^\circ, 0^\circ), (30^\circ, 0^\circ)$ and $(45^\circ, 0^\circ)$. The calculation is realized using a random chosen area of the structure and the transmission spectra are calculated with different incident angles, ϕ , of the light beam. An isotropic photonic bandgap centered at 0.4 is clearly observed, similar to the result shown in Fig. 13.

technique strongly depend on the developing process (Mello et al., 1995), the absorption of photoresists (Rumpf et al., 2004), the mass transport effect (Lai et al., 2006a), and the diffusion of photoacid of negative photoresist (Park et al., 2005). In this Section, we present the use of some existing effect in HL technique to obtain new interesting 2D and 3D structures.

5.1 Recording an interference pattern on a pure photoresist: The absorption effect

The first inherent effect regarding the matter used to record the interference pattern is the absorption. Due to this effect, the exposure dosage decreases along the light propagation, resulting in a non-uniform recorded structure. For photoresist whose absorption coefficient at the excitation wavelength is high, the 2D structures obtained by interference technique will consist of regular material-rods with very limited height and the fabrication of 3D structures by this method is almost impossible.

We consider for example the use of two-beam interference technique for fabrication of material structures. Including the absorption effect of the recorded material, the intensity distribution of a two-beam interference pattern in a sample oriented at angles α and β is expressed as

$$I_\alpha = 2E_0^2 \exp[-2\sigma z / \cos(\theta)] \cos^2[kz \sin \theta \sin \beta + k \cos \theta \cos \beta (x \cos \alpha + y \sin \alpha)], \quad (4)$$

where σ is the absorption coefficient of the photoresist at the excitation wavelength.

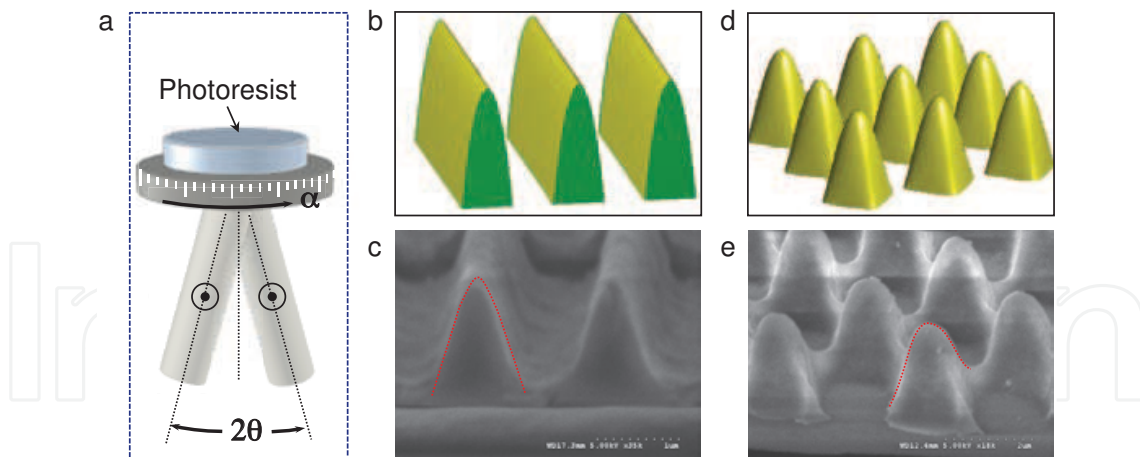


Fig. 15. (a) Experimental arrangement of two-beam interference used for testing the high absorption effect of photoresist. Sample could be rotated by an angle α between different exposures. (b-e) Theoretical calculations and experimental results of 1D (b,c) and 2D (d,e) structures, obtained by using a negative SU8 photoresist and an irradiation light at 325 nm. The structure height (or sample thickness) is limited to about $1.5 \mu\text{m}$ due to the high absorption coefficient of SU8 at 325 nm-wavelength.

Figures 15b and d show the theoretical calculation of the iso-intensity distribution of a two-beam interference pattern obtained with one-exposure (1D) and double-exposure (2D square), respectively. In this case, we used $\sigma = 1656 \text{ cm}^{-1}$ at $\lambda = 325 \text{ nm}$, according to the absorption coefficient, measured experimentally, of the SU8 commercial photoresist (MicroChem Corp.). Due to the high absorption effect of SU8 at the chosen wavelength, the shape of the 1D and 2D structures is different from those obtained without the absorption effect (Lai et al., 2005a;b). The 2D structure for example no longer contain the long cylinders but cylinders-like or cones instead.

The 2D simulated structure resembles the well-known Moth's eye structures (Baker, 1999; Clapham & Hutley, 1973), in which the effective index is increased continuously from 1 to the index of substrate. This kind of structures can be used as an efficient antireflective surface. The two-beam interference therefore can be an useful method to fabricate such kind of photoresist-based antireflective structures with very large area and with adjustable lattice constant and configuration (hexagonal, square, or other).

In order to observe the shape of the fabricated structure, we employed the fabrication setup shown in Fig. 15a, for that the light beam is applied in the back side of the sample, which allows to keep the structure on the substrate after fabrication. The sample is chosen to be very thick (thickness = $10 \mu\text{m}$) to avoid the effect of film thickness on the shape of structure. Figures 15c,e show the structures obtained with one-exposure and double-exposure, respectively, which are in agreement with the theoretical predictions. As consequence of the high absorption of the used photoresist, the structure was formed for a limited height of about $1.5 \mu\text{m}$ and the surface of the cylinder-like was no longer flat instead of a curved shape surface was formed. A Moth's eye structure can be easily obtained by using a simple interference technique.

Note that the combination of high absorption effect and thin film sample (thickness of about $1.5 \mu\text{m}$) allows to obtain neither a 2D perfect cylindrical structure nor Moth's eye structure but a microlens array structure. In addition, the 1D (or 2D) structure could be tilted in any direction by rotating the sample by an angle β , as shown in Section 2, resulting in different

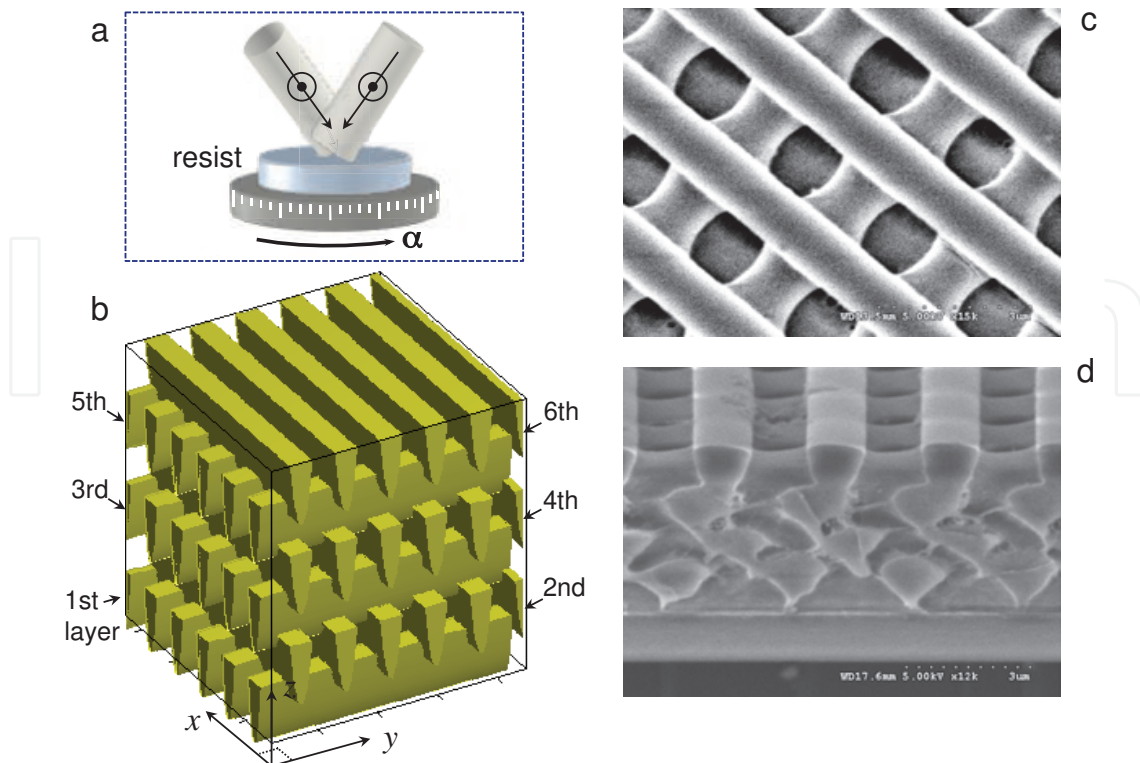


Fig. 16. (a) Experimental arrangement of two-beam interference used for fabrication of desired 3D structure with controllable thickness. (b) Simulation result of a woodpile-like 3D structure obtained by assembling multiple 1D structures. (c) and (d) Top view and side view of an example of a 3D structure consisting of 8 layers, alternatively fabricated in two orthogonal directions. Fabrication was realized by using a negative SU8 photoresist and two-beam interference at 325 nm-wavelength.

kinds of 1D grating such as Blaze-like gratings. Furthermore, 1D or 2D structures obtained by using high absorption effect could be assembled layer by layer to create various 3D structures with no limitation of number of layers.

5.2 Fabrication of desired 3D structures by holographic assembly technique

We have developed a new technique to fabricate 3D desired structure. This technique is based on the high absorption effect and the multi-exposure two-beam interference technique. In fact, under one-exposure, the combination of these two effects allows to obtain a 1D structure with a limited film thickness. By assembling multiple structured layers, layer-by-layer, we then obtained a 3D structures as desired. Each structural layer was obtained by: i) spin-coating the thin film, ii) recording the structure, and iii) post-exposure-baking the sample. Note that the fabrication of top layer doesn't affect the bottom previously recorded layer thanks to the high absorption effect. The desired 3D structure was finally obtained with only one developing process after finishing all fabrications. An example of a simulated woodpile-like 3D structure using a commercial SU8 photoresist exposed at 325 nm-wavelength is shown in Fig. 16b.

Woodpile structure is a simple but very useful lattice with a full PBG (Ozbay et al., 1994). To fabricate such structure, we assembled multiple layers of 1D periodic structure fabricated by one-exposure of two-beam interference pattern. The orientation of 1D structures in two successive layers is changed by 90° , by rotating the sample for two different exposures

(α -angle = 0° and 90°). Figure 16c and d show the top view and side view of a 3D structure obtained by the assembly of 8 layers. The fabricated structures are very uniform for large area, and the structure of each layer is well formed and has no effect on other layers.

We also successfully fabricated other types of 3D structures by rotating the sample by 60° for fabrication of each layer. Similarly, various 3D structures, such as simple cubic or body-centered cubic structures, have been fabricated by assembling multiple 2D structural layers, which are obtained by applying a double-exposure of two-beam interference pattern for each layer. By using this technique, we can therefore assembly multiple 1D and 2D structures, with hexagonal forms or hexagonal and square forms, to obtain many other kinds of 3D structures. It is also possible to assembly multiple 1D structures with different lattice constants in order to obtain bi-photonic crystals with multiple PBG. Furthermore, since the fabrication of the structure in each layer is independent and controlable, we can therefore introduce any kind of defects into desired layer, by using for example the multiphoton polymerization direct laser writing technique or mask-lithography, as presented in Section 3.

5.3 Fabrication of nanovein structures and theoretical analysis of its photonic bandgap

Recently, It has been demonstrated (Park et al., 2005) that the generation and diffusion of photoacid, which acts as a cross-linking agent, depend on the fabrication conditions such as exposure intensity, exposure time, post-exposure bake (PEB), etc. During exposure process, photoinitiator molecules release photoacids in light-exposed regions, and the PEB process accelerates the diffusion of photoacids and induces cationic polymerization of epoxy groups in a negative photoresist. Obviously, with high concentration of photoinitiator molecules and high exposure dosage, it is easy to create a dense polymerized pattern, corresponding to a large size solid structure. Decreasing the concentration of photoinitiator in the photoresist is a simple way to reduce the size of the solid structure. We have developed an original way to fabricate nanostructures by using a mixing of a negative and a positive photoresists. The addition of positive photoresist can reduce the concentration of negative photoresist and thus slow down its polymerization speed.

We mixed S1818, a kind of positive photoresist (Shipley), with SU8 negative photoresist. The fabrication process of using this kind of mixed photoresist is similar to that of pure SU8. The mixing was exposed by a two-beam interference pattern, using a He-Cd laser at $\lambda = 325$ nm. As shown in Fig. 17a, when exposed by the interference pattern, S1818 polymers become monomers and move to the low intensity area while SU8 monomers move to the high intensity area and become polymers. After exposure, the sample was PEB and then developed by Acetone. The developer washed out all S1818 photoresist and SU8 unpolymers. The final result was a solid polymerized SU8 structure. We found that the fabricated structures were solid and smooth, just as those obtained by pure SU8 resist, but the exposure dosage required for obtaining solid structure was much higher than that of pure SU8. Indeed, depending on the volume ratio (VR = ..., 2, 1, 0.5, ...) between SU8 and S1818 photoresists, the exposure time could be varied from ten seconds to few minutes. VR = 2 was an optimum ratio to achieve good structures. The increase of the exposure time required to obtain solid structure is due to the decrease of concentration of SU8 monomers and photoinitiator.

Figures 17b and c show some new structures fabricated by this photoresist mixing and by multiple-exposure two-beam interference technique. The structures are constituted by square [Fig. 17b] or rectangular [Fig. 17c] rods connecting by very narrow veins (< 100 nm). They are totally different to those obtained by pure SU8 photoresist, and do not agree with the

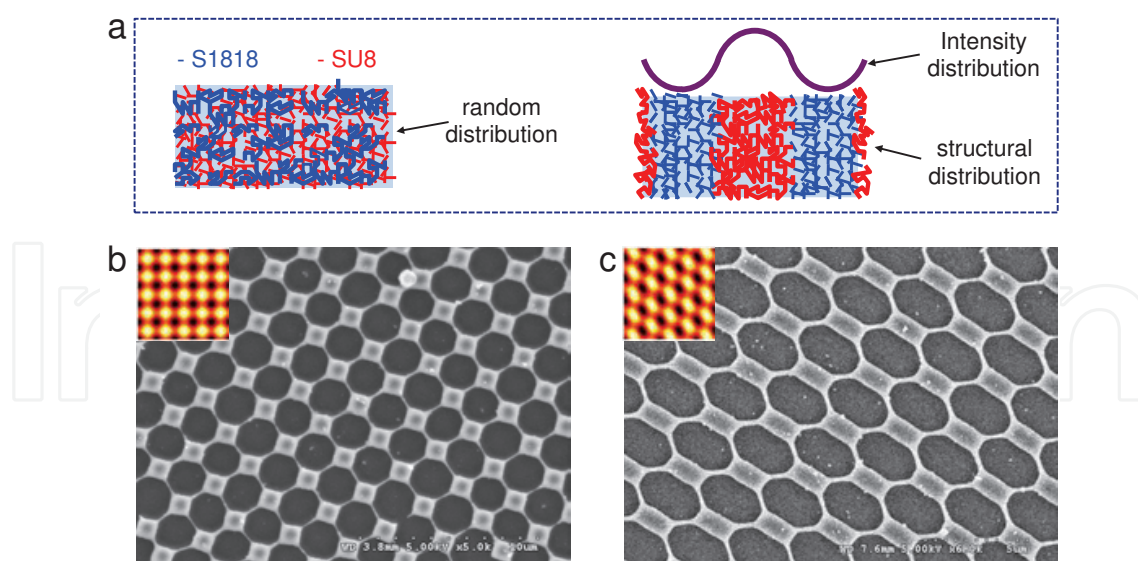


Fig. 17. (a) Illustration of the molecular distribution of the SU8/S1818 mixing. Before exposure, S1818 consists of oligomers and polymers (positive photoresist) and SU8 consists of monomers (negative photoresist). After exposed by the interference pattern, S1818 polymers become monomers and move to the low intensity area while SU8 monomers move to the high intensity area and become polymers. (b) and (c) SEM images of 2D periodic structures obtained with a double-exposure of two-beam interference pattern at different directions. The square or rectangular blocks are connected with narrow veins, thanks to the low concentration of SU8 monomers and the movement of both S1818 and SU8 photoresists. Insets illustrate the simulated structures, same as those shown in Fig. 3, for each experimental result.

theoretical calculations shown in insets of Figs. 17b,c. The result should be a consequence of low concentration of photoinitiator and SU8 monomers. The narrow veins were resulted from high irradiation dosage of each individual exposure (1D) and the square/rectangular rods were due to high irradiation dosage of the combination of two exposures (cross-points of two 1D structures).

This experimental result breaks the well-known HL rule, which usually states that the recorded photoresist structure is a duplication or inverted-duplication of the interference pattern. The result indicates that we need to use the final fabricated structure, not the interference pattern, to calculate optical properties of a PC. Moreover, we show in Fig. 18 that the novel nanovein structures are very useful for PCs applications.

As just mentioned, it is important to use the final fabricated structure as model to calculate the PBG of corresponding PC. Insets of Fig. 18d show a zoom in SEM image of a square unit of the fabricated structure and a corresponding model structure used for the simulation of PBG properties, respectively. The band structures of PCs were calculated by the standard plane-wave expansion method. We first assumed that the PC is constituted of GaAs (dielectric constant $\epsilon = 11.8$) square rods (rod width $R = 0.8a$, a is the lattice constant) connected by nanoveins (vein diameter $D = 0.04a$). It is well known that there is no complete PBG for a standard square 2D PC made by GaAs. However, a complete PBG with a high gap ratio ($\Delta\omega/\omega$) was obtained using this novel square structure. Naturally, this result can be explained by the fact that when the dielectric rods are connected by narrow veins, we achieve a compromise between TE and TM modes, and thus a complete PBG. This argument is similar

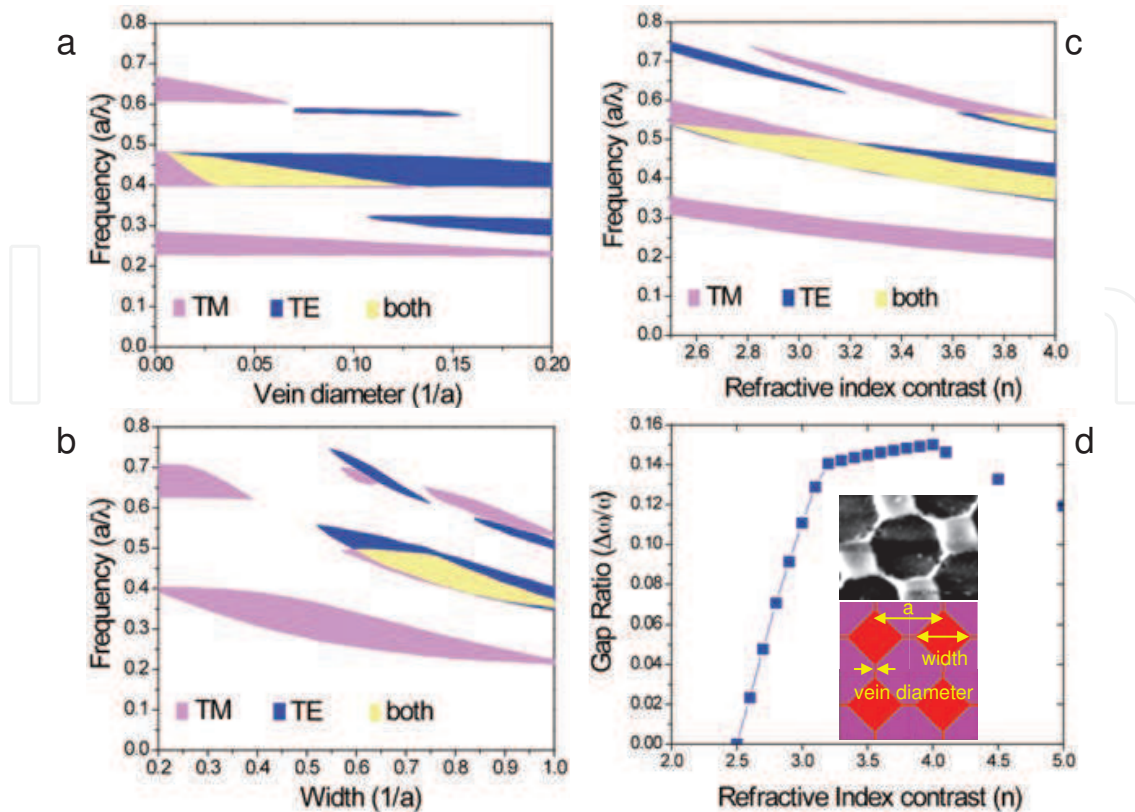


Fig. 18. Simulation results of photonic bandgap (PBG) of a square structure consisting of square rods connecting by nanoveins. (a) Gap map as a function of vein diameter (D), with square rod width $R = 0.8a$. (b) Gap map as a function of square rod width (R), with vein diameter $D = 0.04a$. In (a) and (b), the dielectric constant is assumed to be 11.8 and a is the lattice constant of structure. (c) Gap map as a function of the refractive index contrast, n . Vein diameter and square rod width are chosen to be $D = 0.04a$ and $R = 0.8a$, respectively. (d) Dependence of the normalized absolute PBG ($\Delta\omega/\omega$) on the refractive index contrast. Insets show a zoom in of SEM image and a square unit used for simulations.

to that of the well-known honeycomb structure (Fu et al., 2005). Figures 18a and b show the photonic gap map as a function of R and D ($\epsilon = 11.8$). We can see that a complete PBG can be obtained with a wide range of R (0.6a to 1a) and D (0.005a to 0.125a). The maximum gap ratio was achieved with $R = 0.75a$ and $D = 0.03a$. Note that the optimum parameters are slightly different depending on the dielectric constant of the material. By scanning all possible parameters, we found that the gap ratio can reach 16% with following optimum parameters: $\epsilon = 16$ (Germanium), $R = 0.74a$, and $D = 0.035a$. Figure 18c shows the gap map as a function of the refractive index contrast (n) when $R = 0.8a$ and $D = 0.04a$. The minimum index contrast required for the TE and TM modes to overlap is 2.529 ($\epsilon = 6.4$). Figure 18d shows the dependence of gap ratio of the absolute PBG on the refractive index contrast. The gap ratio increases rapidly when the index contrast varies from 2.53 to 3.2 and it then slightly increases until when n reaches 4. These results are interesting because the new fabricated structure allows to achieve a complete PBG, which is impossible with the traditional square structure.

5.4 Discussions and Conclusions

Interference is an ideal method to fabricate periodic multi-dimensional structures. In this Section, we recognized that there is many influences of fabrication parameters onto the recorded photoresist structures. Those effects traditionally limit the fabrication of desired structures. However, we have studied and used them as new methods to overcome the limitation and create other new and interesting structures, which cannot be obtained by traditional method.

Besides, we have also studied other influences such as mass transport or developing effects. Those effects allow to fabricate for example polymeric microlens arrays (MLAs). Indeed, we have demonstrated that 2D MLAs can be easily fabricated by multi-exposure two-beam interference technique based on the mass transport effect, i.e., diffusion of monomers from unexposed to exposed areas, of SU8 negative photoresist (Wu et al., 2009). The SU8-based MLAs were obtained without transferring to other materials. When using AZ positive photoresist, we have demonstrated a promising method to obtain plastic MLAs with shape- and structure-controlled, by using the combination of double-exposure two-beam interference and plastic replication techniques. Thanks to the developing effect of the positive photoresist, fabricated structures consisting of parabolical, elliptical or hemispherical-shaped concave holes were obtained. These structures were then transferred to plastic MLAs by employing replication and embossing techniques. The fabricated MLAs, with different structures and shapes, can be useful for different applications in optical and display systems such as correction of laser beam profile, aberration, etc.

6. Conclusion

Realization of photonic bandgap materials (photonic crystals) is in high demand for the use in many applications in opto-electronics and photonic domains. In this chapter, simple fabrication techniques based on multiple-exposure of two- or three-beam interference pattern was theoretically and experimentally demonstrated. These techniques have been applied to different kinds of negative and positive photoresists. Various 1D, 2D and 3D periodic and quasi-periodic structures with different configurations were obtained. The structures are perfectly uniform for area as large as 1 cm^2 and with a lattice constant as small as 400 nm. The photonic bandgap of 3D periodic structures is experimentally demonstrated in visible range, which is very promising for many applications. Quasi-periodic structures with very high rotation symmetry level is demonstrated. Its photonic bandgap is theoretically demonstrated to be very isotropic, which cannot be obtained by standard photonic crystal. The experimental results are in well agreement with the theoretical calculations.

Besides, different combination techniques have been proposed in order to embed desired defects, such as waveguide, cavity, etc., into periodic structures. Each method presents its advantage, and can be chosen for the desired applications. Mask-lithography allows to rapidly introduce large defects while multiphoton polymerization direct laser writing creates tiny and arbitrary defects. Moreover, the defect were demonstrated to be embedded in correct position and orientation inside the periodic 2D and 3D structures.

Furthermore, different effects that influence the photoresist-based structures fabricated by interference technique were studied in detail. The high absorption effect limits the height of 2D structures and the thickness of 3D structure. But this effect is demonstrated to be useful for fabrication of other special structures such as moth-eye anti-reflective structure or 3D assembled structure. The control of the monomers and photoinitiators concentration of the used photoresist by mixing two kinds of photoresists allows to obtain new periodic

structures consisting of square or rectangular rods connecting by nanoveins. These structures present complete absolute photonic bandgap at low refractive index contrast, which cannot be obtained by standard photonic crystals.

These studies are very important and useful for the photonic crystal community. It provides a rapid and inexpensive fabrication of large and controllable structures. New structures fabricated by these methods show new optical properties and open the ways for interesting applications.

7. References

- Baker K. M. (1999). Highly corrected close-packed microlens arrays and moth-eye structuring on curved surfaces. *Appl. Opt.*, Vol. 38 (January 2009) 352-356, ISSN 1559-128X.
- Berger, V.; Gauthier-Lafaye, O. & Costard E. (1997). Photonic band gaps and holography. *J. Appl. Phys.*, Vol. 82 (July 1997) 60-64, ISSN 0021-8979.
- Campbell, M.; Sharp, D. N.; Harrison, M. T.; Denning, R. G. & Turberfield A. J. (2000). Fabrication of photonic crystals for the visible spectrum by holographic lithography. *Nature*, Vol. 404 (March 2000) 53-56, ISSN 0028-0836.
- Clapham, P. B. & Hutley, M. C. (1973). Reduction of lens reflection by the Moth eye principle. *Nature*, Vol. 244 (August 1973) 281-282, ISSN 0028-0836.
- Deubel, M.; Freymann, G. V.; Wegener, M.; Pereira, S.; Busch, K. & Soukoulis, C. M. (2004). Direct laser writing of three-dimensional photonic-crystal templates for telecommunications. *Nature Mater.*, Vol. 3 (July 2004) 444-447, ISSN 1476-1122.
- Fu, H. K.; Chen, Y. F.; Chern, R. L. & Chang, C. C. (2005). Connected hexagonal photonic crystals with largest full band gap. *Opt. Express*, Vol. 13 (October 2005) 7854-7860, ISSN 1094-4087.
- Gauthier, R. & Ivanov, A. (2004). Production of quasi-crystal template patterns using a dual beam multiple exposure technique. *Opt. Express*, Vol. 12 (March 2004) 7832-7841, ISSN 1094-4087.
- Inoue, I. & Ohtaka, K. (2004). *Photonic crystals: physics, fabrication and applications*, Springer, Berlin.
- Joannopoulos, J. D.; Meade R. D. & Winn, J. N. (1995). *Photonic crystals: molding the flow of light*, Princeton University Press, Princeton.
- Juodkasis, S.; Mizeikis, V.; Seet, K. K.; Miwa, M. & Misawa, H. (2005). Two-photon lithography of nanorods in SU-8 photoresist. *Nanotechnology*, Vol. 16 (April 2005) 846-849, ISSN 0957-4484.
- Kawata, S.; Sun, H.-B.; Tanaka, T. & Takada, K. (2001). Finer features for functional microdevices. *Nature*, Vol. 412 (August 2001) 697-698, ISSN 0028-0836.
- Lai, N. D.; Liang, W. P.; Lin, J. H.; Hsu, C. C. & Lin, C. H. (2005). Fabrication of two- and three-dimensional periodic structures by multi-exposure of two-beam interference technique. *Opt. Express*, Vol. 13 (November 2005) 9605-9611, ISSN 1094-4087.
- Lai, N. D.; Liang, W. P.; Lin, J. H. & Hsu, C. C. (2005). Rapid fabrication of large-area periodic structures containing well-defined defects by combining holography and mask techniques. *Opt. Express*, Vol. 13 (July 2005) 5331-5337, ISSN 1094-4087.
- Lai, N. D.; Lin, J. H.; Liang, W. P.; Hsu, C. C. & Lin, C. H. (2006). Precisely introducing defects into periodic structures by using a double-step laser scanning technique. *Appl. Opt.*, Vol. 45 (August 2006) 5777-5782, ISSN 1559-128X.

- Lai, N. D.; Lin, J. H.; Huang, Y. Y. & Hsu, C. C. (2006). Fabrication of two- and three-dimensional quasi-periodic structures with 12-fold symmetry by interference technique. *Opt. Express*, Vol. 14 (October 2006) 10746-10752, ISSN 1094-4087.
- Lai, N. D.; Lin, J. H. & Hsu, C. C. (2007). Realization of highly rotational symmetric quasi-periodic structures by multi-exposure of three-beam interference technique. *Appl. Opt.*, Vol. 46 (August 2007) 5645-5648, ISSN 1559-128X.
- Lai, N. D.; Huang, Y. D.; Do, D. B.; Lin, J. H. & Hsu, C. C. (2009). Fabrication of periodic nanovein structures by holography lithography technique. *Opt. Express*, Vol. 17 (March 2009) 3362-3369, ISSN 1094-4087.
- Lai, N. D.; Zheng, T. S.; Do, D. B.; Lin, J. H. & Hsu, C. C. (2010). Fabrication of desired three-dimensional structures by holographic assembly technique. *Appl. Phys. A*, Vol. 100 (July 2010) 171-175, ISSN 0947-8396.
- Mello, B. A.; Costa, I. F.; Lima, C. R. A. & Cescato, L. (1995). Developed profile of holographically exposed photoresist gratings. *Appl. Opt.*, Vol. 34 (February 1995) 597-603, ISSN 1559-128X.
- Noda, S; Fujita M. & Asano T. (2007). Spontaneous-emission control by photonic crystals and nanocavities. *Nature Photon.*, Vol. 1 (August 2007) 449-458, ISSN 1749-4885.
- Park, S. H.; Lim, T. W.; Yang, D. Y.; Cho, N. C. & Lee, K. S. (2006). Fabrication of a bunch of sub-30-nm nanofibers inside microchannels using photopolymerization via a long exposure technique. *Appl. Phys. Lett.*, Vol. 89 (October 2006) 173133, ISSN 0003-6951.
- Ozby, E.; Abeyta, A.; Tuttle, G.; Tringides, M.; Biswas, R.; Soukoulis, C.; Chan, C. & Ho, K. (1994). Measurement of a three-dimensional photonic band gap in a crystal structure made of dielectric rods. *Phys. Rev. B*, Vol. 50 (July 1994) 1945-1948, ISSN 1098-0121.
- Rinne, S. A.; Garcia-Santamaria, F. & Braun, P. V. (2008). Embedded cavities and waveguides in three-dimensional silicon photonic crystals. *Nature Photon.*, Vol. 2 (December 2007) 52-56, ISSN 1749-4885.
- Rumpf, R. C. & Johnson, E. G. (2004). Fully three-dimensional modeling of the fabrication and behavior of photonic crystals formed by holographic lithography. *J. Opt. Am. Soc. A*, Vol. 21 (September 2004) 1703-1713, ISSN 1084-7529.
- Sakoda, K. (2001). *Optical properties of photonic crystals*, Springer, Berlin.
- Sibilia, C.; Benson, T. M.; Marciniak, M. & Szoplik, T. (Eds.) (2008). *Photonic crystals: physics and technology*, Springer, ISBN 978-88-470-0843-4, Berlin.
- Sun, H. B.; Matsuo, S. & Misawa, H. (1999). Three-dimensional photonic crystal structures achieved with two-photon-absorption photopolymerization of resin. *Appl. Phys. Lett.*, Vol. 74 (February 1999) 786-788, ISSN 0003-6951.
- Yablonovitch, E. (1987). Inhibited spontaneous emission in solid-state physics and electronics. *Phys. Rev. Lett.*, Vol. 58 (May 1987) 2059-2062, ISSN 0031-9007.
- Wang, X.; Ng, C. Y.; Tam, W. Y.; Chan, C. T. & Sheng, P. (2003). Large-area two-dimensional mesoscale quasi-crystals. *Adv. Mater.*, Vol. 15 (September 2003) 1526-1528, ISSN 0935-9648.
- Wong, S.; Kitaev, V. & Ozin, G. A. (2003). Colloidal crystal films: advances in universality and perfection. *J. Am. Chem. Soc.*, Vol. 125 (November 2003) 15589-15598, ISSN 0002-7863.
- Wu, C. Y.; Lai, N. D. & Hsu, C. C. (2008). Rapidly self-assembling three-dimensional opal photonic crystals. *J. Korean Phys. Soc.*, Vol. 52 (May 2008) 1585-1588, ISSN 0374-4884.
- Wu, C. Y.; Chiang, T. H.; Lai, N. D.; Do, D. B. & Hsu, C. C. (2009). Fabrication of SU-8 microlens arrays by multi-exposure two-beam interference technique. *Appl. Opt.*, Vol. 48 (May 2009) 2473-2479, ISSN 1559-128X.

Zoorob, M. E.; Charlton, M. D. B.; Parker, G. J.; Baumberg, J. J. & Netti, M. C. (2000). Complete photonic bandgaps in 12-fold symmetric quasicrystals. *Nature*, Vol. 404 (April 2000) 740-743, ISSN 0028-0836.

IntechOpen

IntechOpen



Holography, Research and Technologies

Edited by Prof. Joseph Rosen

ISBN 978-953-307-227-2

Hard cover, 454 pages

Publisher InTech

Published online 28, February, 2011

Published in print edition February, 2011

Holography has recently become a field of much interest because of the many new applications implemented by various holographic techniques. This book is a collection of 22 excellent chapters written by various experts, and it covers various aspects of holography. The chapters of the book are organized in six sections, starting with theory, continuing with materials, techniques, applications as well as digital algorithms, and finally ending with non-optical holograms. The book contains recent outputs from researches belonging to different research groups worldwide, providing a rich diversity of approaches to the topic of holography.

How to reference

In order to correctly reference this scholarly work, feel free to copy and paste the following:

Ngoc Diep Lai, Jian Hung Lin, Danh Bich Do, Wen Ping Liang, Yu Di Huang, Tsao Shih Zheng, Yi Ya Huang, Chia Chen Hsu (2011). Fabrication of Two- and Three-Dimensional Photonic Crystals and Photonic Quasi-Crystals by Interference Technique, Holography, Research and Technologies, Prof. Joseph Rosen (Ed.), ISBN: 978-953-307-227-2, InTech, Available from: <http://www.intechopen.com/books/holography-research-and-technologies/fabrication-of-two-and-three-dimensional-photonic-crystals-and-photonic-quasi-crystals-by-interferen>

INTECH
open science | open minds

InTech Europe

University Campus STeP Ri
Slavka Krautzeka 83/A
51000 Rijeka, Croatia
Phone: +385 (51) 770 447
Fax: +385 (51) 686 166
www.intechopen.com

InTech China

Unit 405, Office Block, Hotel Equatorial Shanghai
No.65, Yan An Road (West), Shanghai, 200040, China
中国上海市延安西路65号上海国际贵都大饭店办公楼405单元
Phone: +86-21-62489820
Fax: +86-21-62489821

© 2011 The Author(s). Licensee IntechOpen. This chapter is distributed under the terms of the [Creative Commons Attribution-NonCommercial-ShareAlike-3.0 License](#), which permits use, distribution and reproduction for non-commercial purposes, provided the original is properly cited and derivative works building on this content are distributed under the same license.

IntechOpen

IntechOpen